

Preparation of nanocrystalline cubic ZrO₂ with different shapes via a simple precipitation approach

Sahar Zinatloo-Ajabshir¹ · Masoud Salavati-Niasari¹

Received: 28 October 2015 / Accepted: 18 December 2015 / Published online: 29 December 2015
© Springer Science+Business Media New York 2015

Abstract In this study, Triethylenetetramine (Trien) was employed not only as precipitator, but also as morphology- and size-modifier to prepare pure cubic zirconium dioxide nanocrystals. Trien with high steric hindrance effect was employed as morphology- and size-modifier. Besides Trien as novel precipitator, zirconyl nitrate was employed as zirconium source for the synthesis of pure cubic zirconium dioxide nanocrystals through a facile surfactant-free precipitation process. SEM results of this investigation reveal that grain size and shape of the zirconium dioxide powders can be modified by changing key preparation factors such as the solvent sort, precipitator concentration and reaction time. XRD, FESEM, DR–UV–vis, PL, FT-IR and EDX were used to characterize the as-produced zirconium dioxide nanocrystals. Moreover, the photocatalytic performance of as-prepared zirconium dioxide nanocrystals was evaluated by degradation of erythrosine dye as a model of water pollutant.

1 Introduction

During the past decades, the preparation of nanomaterials has attracted broad attention owing to their unique applications in different areas [1–4]. Among these nano-sized materials, zirconia as an remarkable metal oxide has been paid particular attention for a long time owing to its noteworthy optical and electrical features as well as advantageous applications in the preparation of the

transparent optical devices, electrochemical capacitor electrodes, fuel cells and catalysts [5–11]. Zirconium dioxide has three crystal forms that are stabilized at different temperature ranges: monoclinic (below 1170 °C), tetragonal (1170–2370 °C), and cubic (2370–2680 °C) [12]. Until now, several ways have been developed to synthesize ZrO₂, including sol–gel [13], hydrothermal [14], thermal decomposition [15], microwave irradiation [16], precipitation [12, 17], and sonochemical [18, 19]. Since particle size and shape have substantial influence on the features and usages of the nanoscale materials, several ways have been presenting for particle size and morphology modified preparation of nanoscale materials [20–29]. Here, zirconium dioxide nanocrystals are synthesized through a facile surfactant-free precipitation way by applying triethylenetetramine (Trien) and zirconyl nitrate. The precipitation way as a simple and reliable preparation procedure provides a promising route to the homogeneous nanomaterials preparation. This research is the first successful effort for the large-scale preparation of pure cubic zirconium dioxide nanocrystals by applying triethylenetetramine (Trien) through a surfactant-free precipitation way. The influences of several preparation factors on the size and shape of zirconium dioxide are also studied.

2 Experimental

2.1 Materials and characterization

Zirconium dioxide nanocrystals were synthesized, employing the following reagents, purchased from Merck Company: zirconyl nitrate (ZrO(NO₃)₂·6H₂O (ZN), CH₂OHCH₂OH (EG), triethylenetetramine (Trien), CH₂OHCH₂CH₂OH (PG), ethylenediamine (en) and methanol

✉ Masoud Salavati-Niasari
salavati@kashanu.ac.ir

¹ Institute of Nano Science and Nano Technology, University of Kashan, P. O. Box. 87317-51167, Kashan, I. R. Iran

(CH₃OH). The morphological features of the zirconium dioxide nanocrystals were evaluated by two field-emission scanning electron microscopes (Hitachi s4160, Japan and Tescan mira3, cheque). Fourier transform infrared spectra of as-prepared samples were recorded employing KBr pellets on a FT-IR spectrometer (Magna-IR, 550 Nicolet). The electronic spectra of the zirconium dioxide nanocrystals were taken on a Scinco UV–vis scanning spectrometer (Model S-4100). GC-2550TG (Teif Gostar Faraz Company, Iran) were used for all chemical analyses. The EDS analysis of the as-obtained zirconium dioxide nanocrystals was performed by a Philips XL30 microscope. Room temperature photoluminescence (PL) analysis of the as-prepared zirconium dioxide nanocrystals was carried out by a Perkin Elmer (LS 55) fluorescence spectrophotometer. The X-ray diffraction (XRD) patterns of as-prepared samples were collected with a Philips diffractometer employing X'PertPro and the monochromatized Cu K α radiation ($\lambda = 1.54 \text{ \AA}$). The detailed morphological features of zirconium dioxide nanocrystals were investigated by a JEM-2100 transmission electron microscope (TEM) with an accelerating voltage of 200 kV.

2.2 Preparation of zirconium dioxide nanocrystals

Zirconium dioxide nanocrystals were synthesized by simple precipitation way. To prepare sample no. 1, 1 mmol of Trien was dissolved in 30 cm³ of distilled water and then was added drop-wise to 30 cm³ solution containing 1 mmol of zirconyl nitrate under magnetic stirring for 10 min. The white hydroxide precipitate was filtered and washed with distilled water for three times. The zirconium dioxide nanocrystals were prepared after drying at 80 °C and calcining of as-obtained hydroxide precipitate at 600 °C during 4 h (Fig. 1). A blank test was performed by applying en instead of Trien to evaluate the effect of the Trien. The effects of solvent sort, concentration of Trien and reaction time on the shape and the size of the zirconium dioxide powders were evaluated and the obtained results exhibited in Table 1.

2.3 Photocatalytic test

The photocatalytic features of as-synthesized zirconium dioxide nanocrystals were evaluated by applying erythrosine dye solution in the quartz reactor (the solution including 0.001 g of the erythrosine and 0.04 g of the



Fig. 1 Schematic depicting the preparation of nano zirconium dioxide powders

zirconium dioxide nanocrystals). After aerating for 1/2 h, the mixture was subjected to the illumination of the UV light. The erythrosine photodegradation percentage was determined as follow:

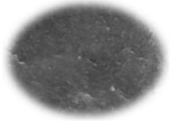
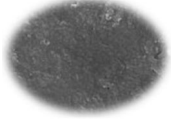
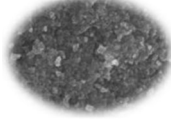
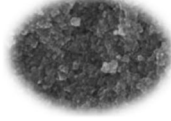
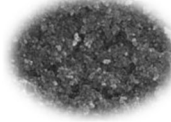
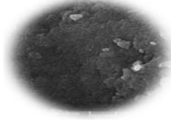
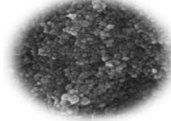
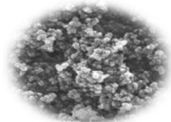
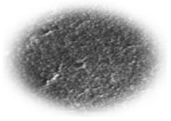
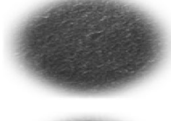
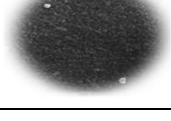
$$D.P.(t) = \frac{A_0 - A_t}{A_0} \times 100 \quad (1)$$

where A_t and A_0 are the measured absorbance quantity of the erythrosine solution at t and 0 min by a UV–vis spectrometry.

3 Results and discussion

To characterize the phase and crystal structure of the as-obtained zirconium dioxide nanocrystals, XRD method was applied. XRD patterns of the sample no. 5 after washing phase, and after calcination are exhibited in Fig. 2a, b. Figure 2a clearly demonstrates that the hydroxide precipitate synthesized by the precipitation way (after washing phase) is amorphous. The diffraction peaks

Table 1 Various reaction conditions for formation of nano zirconium dioxide powders

Sample no.	Precipitator	Molar ratio (precipitator: $ZrO(NO_3)_2 \cdot xH_2O$)	Solvent	Time (min)	SEM
1	Trien	1:1	H ₂ O	0	
2	Trien	2:1	H ₂ O	0	
3	Trien	3:1	H ₂ O	0	
4	Trien	4:1	H ₂ O	0	
5	Trien	5:1	H ₂ O	0	
6 ^a	en	10:1	H ₂ O	0	
7	Trien	5:1	H ₂ O	20	
8	Trien	5:1	H ₂ O	40	
9	Trien	5:1	H ₂ O/Methanol (25/75)	0	
10	Trien	5:1	H ₂ O/EG(25/75)	0	
11	Trien	5:1	H ₂ O/PG(25/75)	0	

^a Blank test, in the absence of Trien

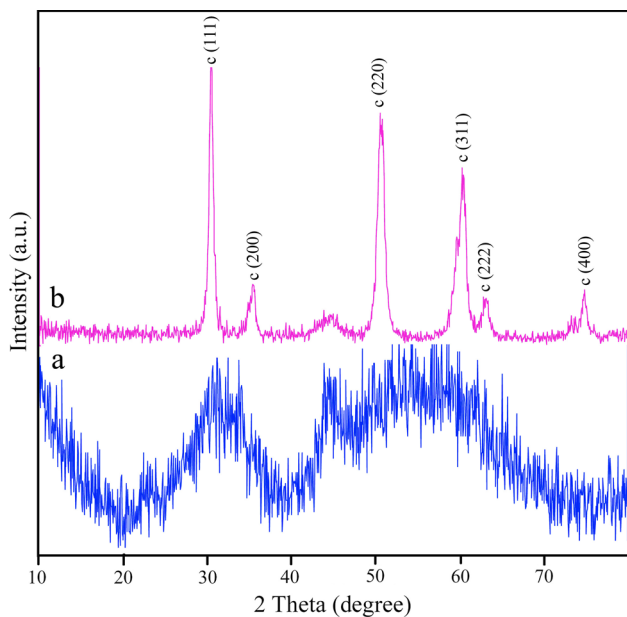


Fig. 2 XRD patterns of sample no. 5 after washing *a*, and after calcination *b*

at 30.41, 35.37, 50.81, 60.49, 63.03 and 74.69 degree, which correspond to the (111), (200), (220), (311), (222) and (400) planes, are well-matched to a pure cubic phase of ZrO_2 . The intensities and positions of the peaks are in agreement with the literature (JCPDF card no. 03-0640). Utilizing Sherrer equation [25], the average crystallite size

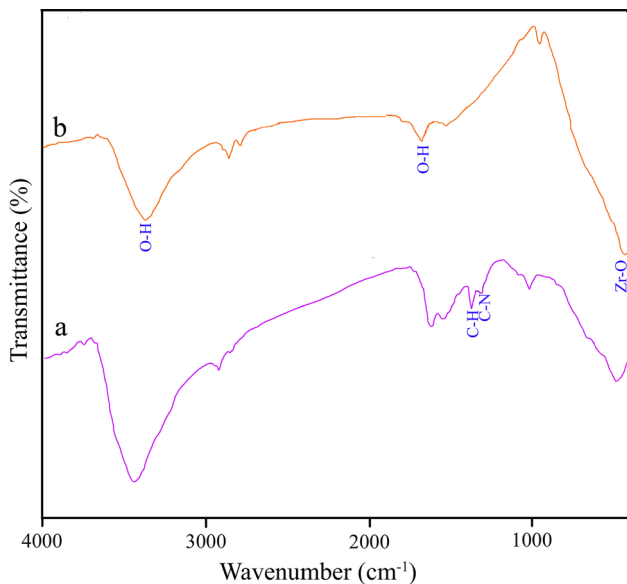


Fig. 3 FT-IR spectra of sample no. 5 after washing *a*, and after calcination *b*

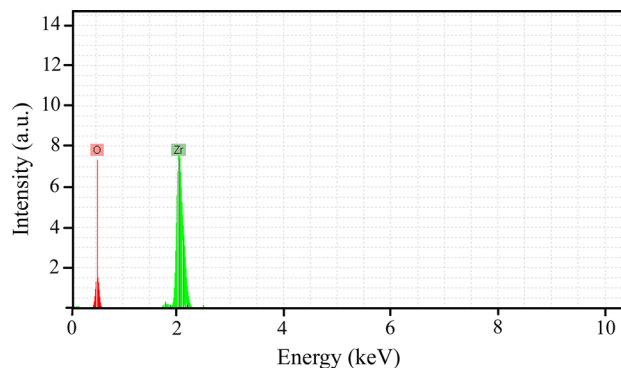


Fig. 4 EDS pattern of nano zirconium dioxide powders (sample no. 5)

of the obtained zirconia from the XRD results was estimated to be about 20 nm.

Figure 3 reveals FT-IR spectra of sample no. 5 after washing phase and after calcination. The (C–N) stretching vibration band at 1341 cm^{-1} and (C–H) bending vibration band 1383 cm^{-1} illustrate the presence of Trien (Fig. 3a). They perfectly vanish after calcination phase. The presence of physisorbed water molecules linked to zirconium dioxide nanocrystals [30] is demonstrated by the absorption peaks located at 3432 and 1629 cm^{-1} which are assigned to the $\nu(\text{OH})$ stretching and bending vibrations, respectively. The band at 499 cm^{-1} is corresponding to the characteristic peak of zirconia (Zr–O vibration) which illustrate the synthesis of zirconia [17] (Fig. 3b).

The chemical composition and purity of as-produced zirconium dioxide nanocrystals were examined by the EDS, and the results are illustrated in Fig. 4. In the EDS spectrum of sample no. 5, only the characteristic peaks of Zr and O are observed. No peak of any impurity was detected, demonstrating the high purity of the product.

The shape and particle size of nano zirconium dioxide powders (sample no. 5) was additional evaluated by TEM. Figure 5 illustrates TEM image of the sample no. 5. As seen, the zirconium dioxide nanoparticles with quasi-spherical shape are sintered together. The TEM image also reveals that as-synthesized nanoparticles have diameter from 30 to 50 nm.

The optical features of as-synthesized nano zirconium dioxide powders (sample no. 5) were examined by PL and DR–UV–vis techniques. Figure 6a reveals the DR–UV–vis spectrum of sample no. 5. It illustrates the absorption band at 338 nm. The energy gap (E_g) can be evaluated based on the DR–UV–vis results applying Tauc’s relationship [31].

$$(Ah\nu)^n = B(h\nu - E_g) \tag{2}$$

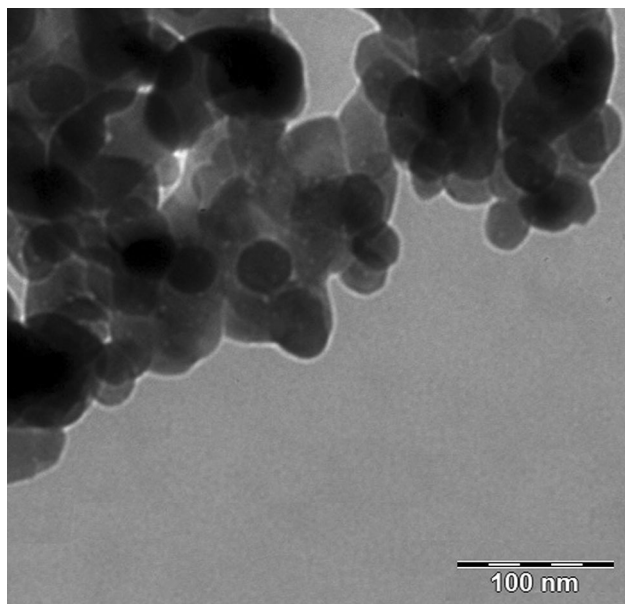


Fig. 5 TEM image of nano zirconium dioxide powders (sample no. 5)

where A is absorbance quantity, n is 2 or 1/2 for direct and not direct transitions, $h\nu$ is the energy of the photon and B is a substance constant. The E_g quantity of the nano zirconium dioxide powders as direct semiconductor substance was determined with extrapolating the lineal part of the plot of $(\alpha h\nu)^2$ against $h\nu$ to the axis of energy (inset in Fig. 6a). The E_g quantity of the zirconium dioxide nanocrystals calculated to be 3.4 eV.

Figure 6b reveals the PL spectrum of the as-prepared zirconium dioxide nanocrystals (sample no. 5). The emission peak at nearly 481 nm is appeared in the PL spectrum (excitation wavelength = 325 nm). This appeared emission peak can be assigned to the electron transitions in intrinsic defects of zirconium dioxide nanocrystals, which is analogous to the previous reports [32–37].

Photodegradation of erythrosine dye as a model of water pollutant under UV light illumination was applied to evaluate the features of the as-obtained zirconium dioxide nanocrystals (sample no. 5). Figure 6c presents the obtained result. No erythrosine dye was practically deleted after 2 h without applying UV light illumination or as-synthesized zirconium dioxide nanocrystals owing to the

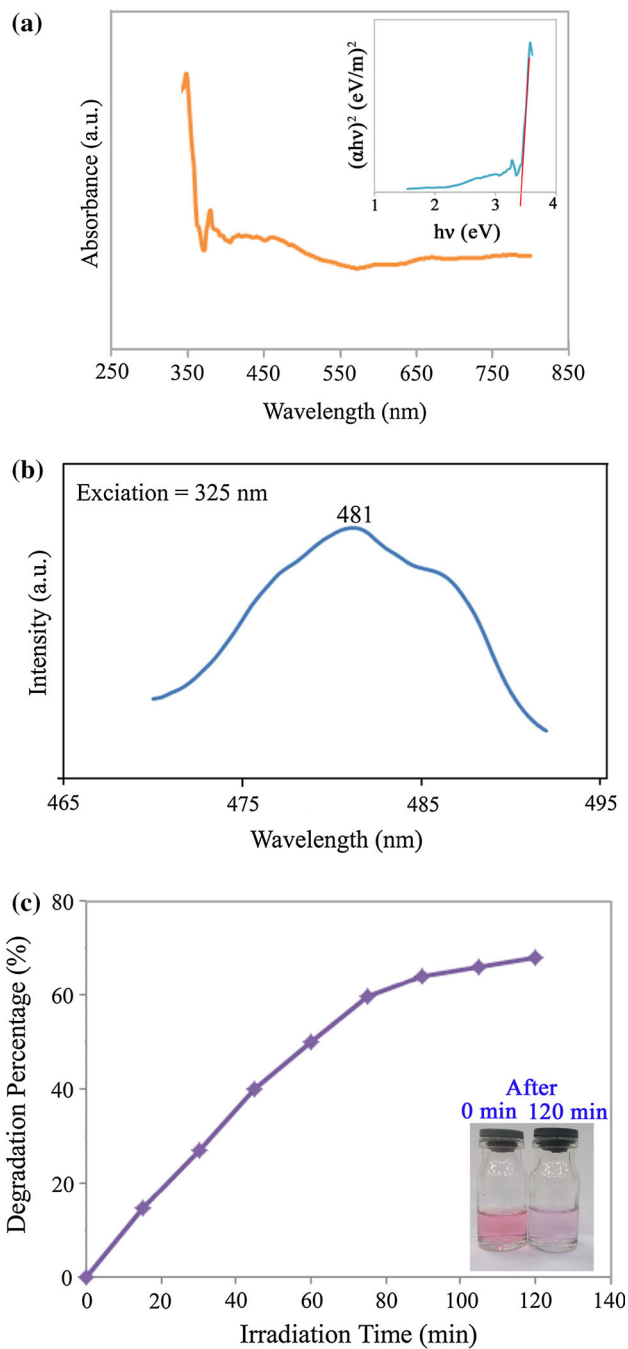


Fig. 6 DR-UV-vis spectrum (a), PL spectrum (b) of the sample no. 5 (inset: the curve of $(\alpha h\nu)^2$ against $h\nu$) and photocatalytic erythrosine degradation of nano zirconium dioxide powders (sample no. 5) under UV light (c)

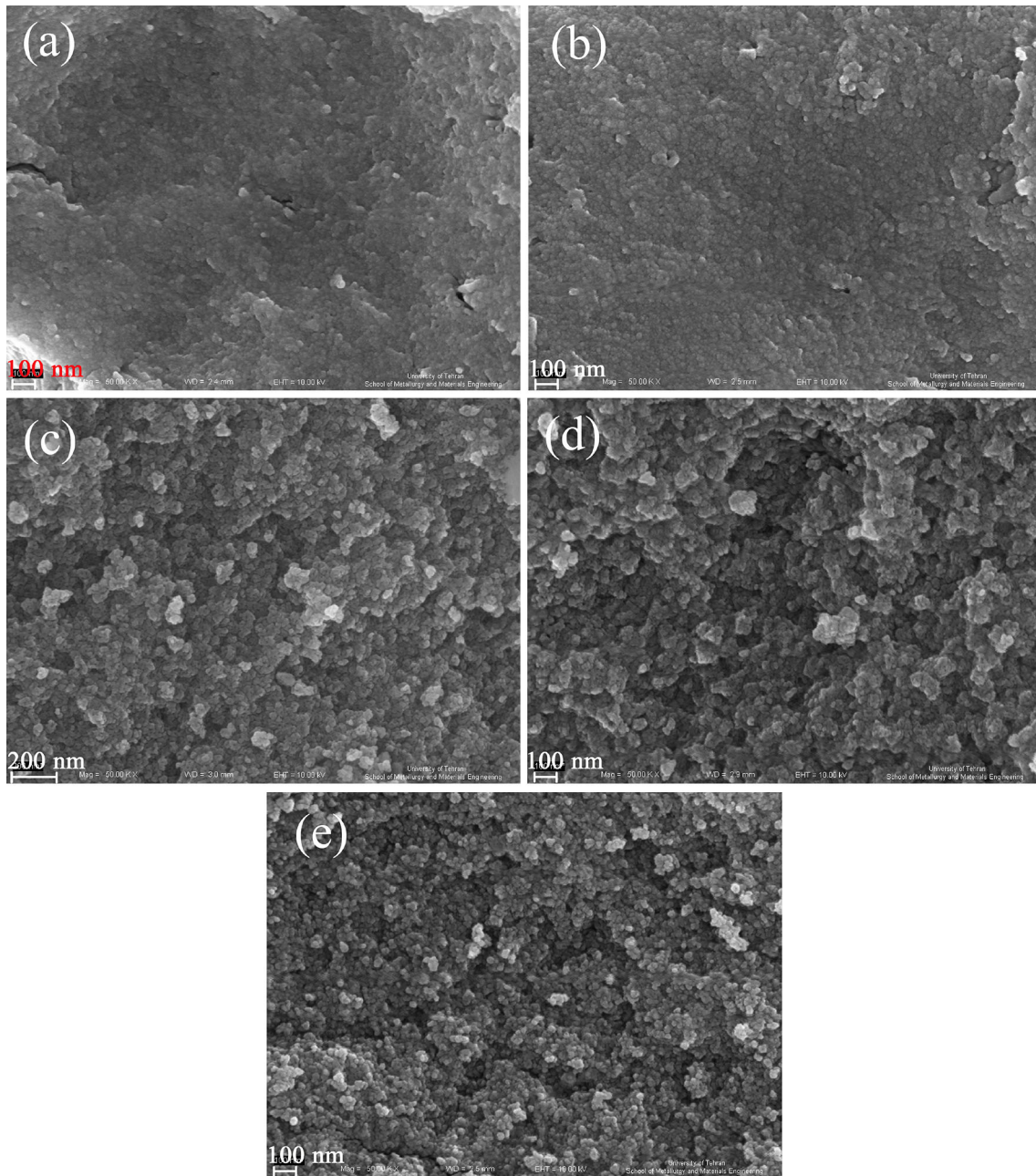


Fig. 7 FESEM images of **a** sample no. 1, **b** sample no. 2, **c** sample no. 3, **d** sample no. 4, and **e** sample no. 5

insignificant contribution of the self-degradation. With utilizing photocatalytic calculations by Eq. (1), the erythrosine dye degradation percentage was about 68 after 2 h illumination of UV light. This obtained photocatalytic

result indicates that as-produced zirconium dioxide nanocrystals have very good capability to be employed as convenient and appropriate nanostructured substance for photocatalytic usages under UV light.

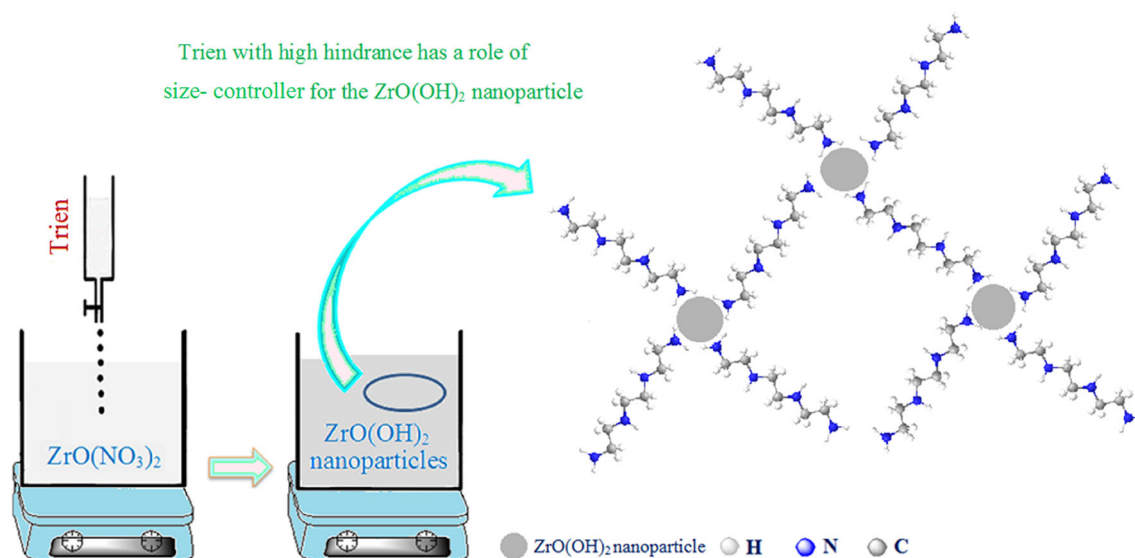


Fig. 8 Schematic illustration of the mechanism effect of the Trien for preparation of the nano zirconium dioxide powders

FESEM method was applied to evaluate the influences of several preparation factors on the morphological features of the nano zirconium dioxide powders.

3.1 Influence of Trien concentration

To evaluate the influence of Trien concentration on the shape of the zirconium dioxide powders, FESEM images of samples nos. 1–5 prepared by employing 1:1, 2:1, 3:1, 4:1 and 5:1 molar ratios of Trien to ZN were obtained and exhibited in Fig. 7a–e, respectively. As already described, the initiative of this study compared to other studies is that for the preparation of zirconium dioxide nanocrystals, Trien as a novel precipitating agent was employed, without applying external capping agent. Trien played precipitating agent as well as morphology- and size-modifier role. The Trien can precipitate zirconyl hydroxide from zirconyl nitrate and may hinder the aggregation of obtained zirconyl hydroxide nanoparticles as morphology- and size-modifier (Fig. 8). It seems that nucleation process to be taken place rather than the particle growth process owing to the presence of Trien with very good steric hindrance influence. Several molar ratios of Trien to ZN were employed to evaluate Trien concentration effect on zirconium dioxide powders shape. When 1:1 and 2:1 molar ratios of Trien to ZN

were employed, zirconium dioxide powders with the dense agglomerated particle-like structures were obtained (Fig. 7a, b). As exhibited in Fig. 7c–e, by increasing the molar ratio from 2:1 to 5:1, nano zirconium dioxide powders with spherical shape were prepared (Fig. 7c–e). It seems that the possibility of collision between prepared zirconyl hydroxide nanoparticles is decreased when Trien dosage increases, owing to the presence of Trien with very good steric hindrance influence. Amongst these employed concentration of Trien, nano zirconium dioxide powders with very homogeneous spherical shape and with small grain size (sample no. 5) can be prepared by employing 5 mmol of Trien. As seen, with less concentration of Trien (3 and 4 mmol), nano zirconium dioxide powders with not uniform spherical morphology can be prepared that are highly aggregated in some places (Fig. 7c, d). So, the Trien dosage has important impact on the particle size and shape of zirconium dioxide powders.

3.2 Influence of Trien

The influence of the Trien on the particle size and shape of the zirconium dioxide powders was evaluated (Fig. 9). For gain this aim, sample no. 6 was obtained as blank test employing en. FESEM image of sample no. 6 is

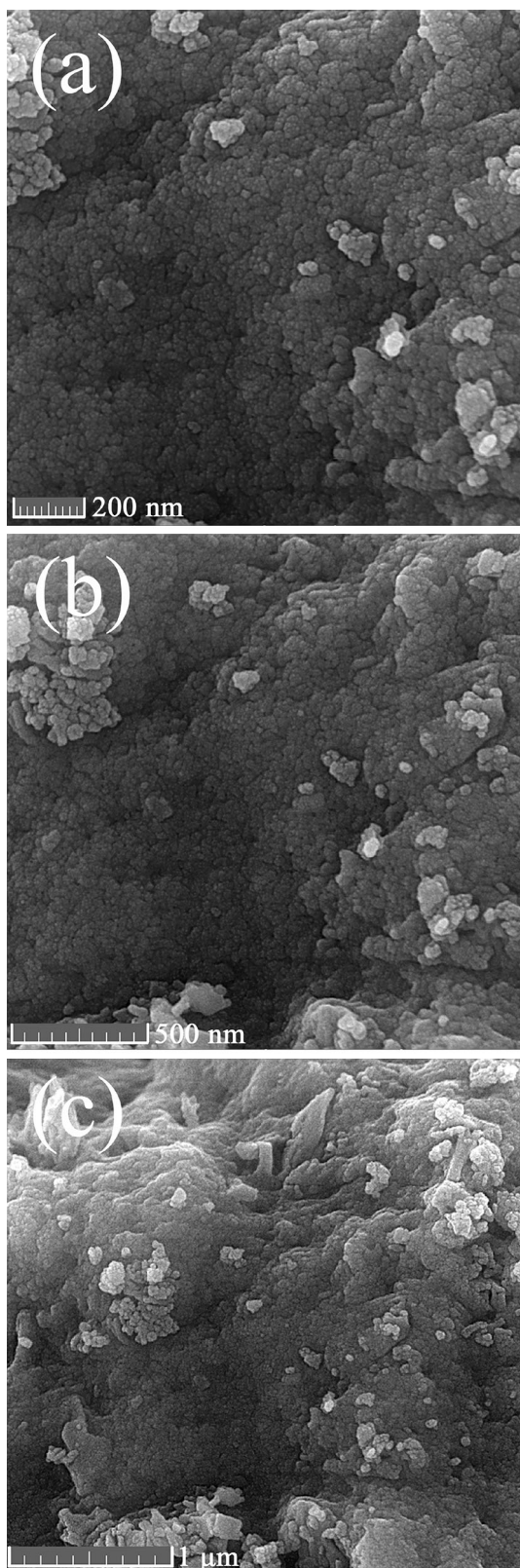


Fig. 9 FESEM images of the sample no. 6

exhibited in Fig. 9. It can be seen that in the absence of Trien, zirconium dioxide powders with irregular particle-like structures with high agglomeration were formed. As described, by employing Trien (Fig. 7e), the collision possibility between prepared zirconyl hydroxide nanoparticles decreased owing to the presence of Trien with very good steric hindrance influence, and consequently the grain size of zirconium dioxide lessened. These results demonstrate that Trien with high steric hindrance effect is an appropriate morphology- and size-modifier to prepare nano zirconium dioxide powders with uniform spherical shape and with small grain size.

3.3 Influence of reaction time

In order to evaluate the influence of reaction time factor on the morphology of zirconium dioxide powders, two reactions were carried out by employing 5 mmol of Trien for 1/3 and 2/3 h. Figure 10a, b reveals FESEM images of the samples prepared for 1/3 and 2/3 h, respectively. It was observed that with increasing time from 0 to 1/3 h (sample no. 7) (Fig. 10a) and 2/3 h (sample no. 8) (Fig. 10b), nano zirconium dioxide powders with irregular spherical morphology and with large grain size were formed.

3.4 Influence of solvent

Moreover, the effect of solvent type on the particle size and shape of the zirconium dioxide powders was evaluated. Figure 11 reveals FESEM images of the zirconium dioxide powders prepared by employing 5 mmol of Trien for 0 min with different solvents via precipitation way. In the presence of water as solvent, nano zirconium dioxide powders with uniform spherical shape are formed (Fig. 7e). As exhibited in Fig. 11a–f, by employing the CH_3OH , $\text{CH}_2\text{OHCH}_2\text{OH}$ and $\text{CH}_2\text{OHCH}_2\text{CH}_2\text{OH}$ as solvent, the morphology of as-prepared zirconium dioxide powders changes from uniform spherical to the dense agglomerated particle-like. The $\text{CH}_2\text{OHCH}_2\text{OH}$ and $\text{CH}_2\text{OHCH}_2\text{CH}_2\text{OH}$ with polar agents can cover the nuclei in all dimensions and limit them from additional growing in all directions and consequently hinder the production of nano zirconium dioxide powders with uniform spherical shape (Fig. 12).

The proposed preparation mechanism of pure cubic zirconium dioxide nanocrystals employing Trien can be explained as follows:

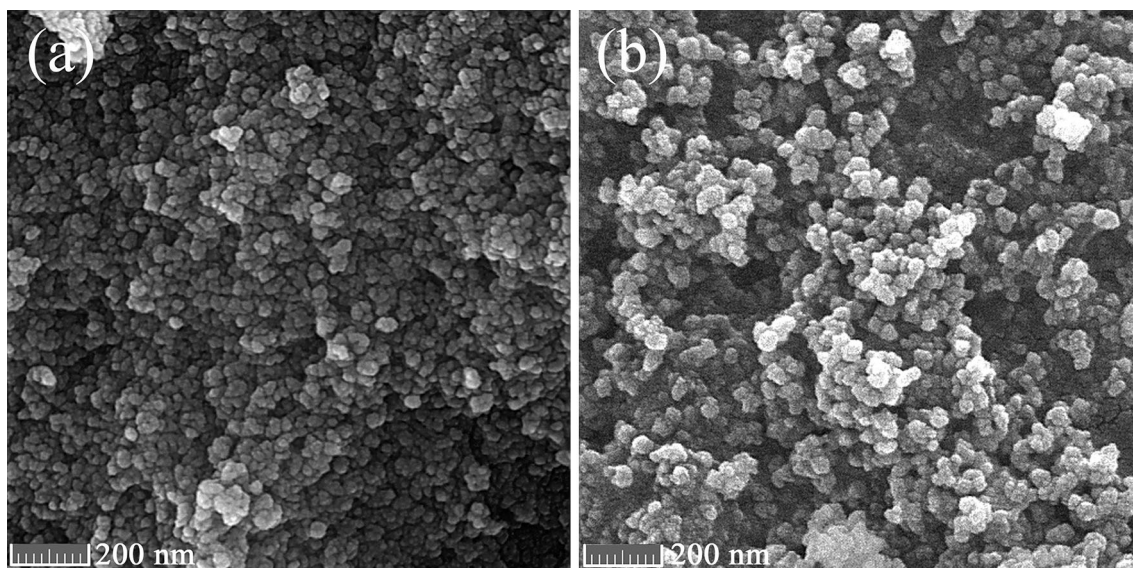
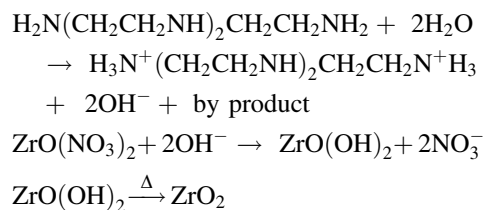


Fig. 10 FESEM images of **a** sample no. 7, and **b** sample no. 8



4 Conclusions

In summary, pure cubic nano zirconium dioxide powders with homogeneous spherical shape has been successfully synthesized from zirconyl nitrate and triethylenetetramine (Trien) through a facile and low-cost precipitation way. By altering the reaction time,

solvent type and precipitator concentration, we could synthesize nano zirconium dioxide powders with very homogeneous spherical morphology and with small grain size. Employing of Trien as a precipitating agent as well as morphology- and size-modifier is the novelty of this work. This study reveals that Trien is an excellent choice for synthesis of nano zirconium dioxide powders without employing any external surfactants. The optical features of the as-obtained zirconium dioxide nanocrystals were also evaluated. The as-produced zirconium dioxide nanocrystals may be applied as convenient and appropriate nanostructured substance for photocatalytic usages under UV light such as elimination of erythrosine dye, since the erythrosine dye photodegradation was obtained to be 68 % within 2 h.

Fig. 11 FESEM images of **a**, **b** sample no. 9, **c**, **d** sample no. 10, and **e**, **f** sample no. 11

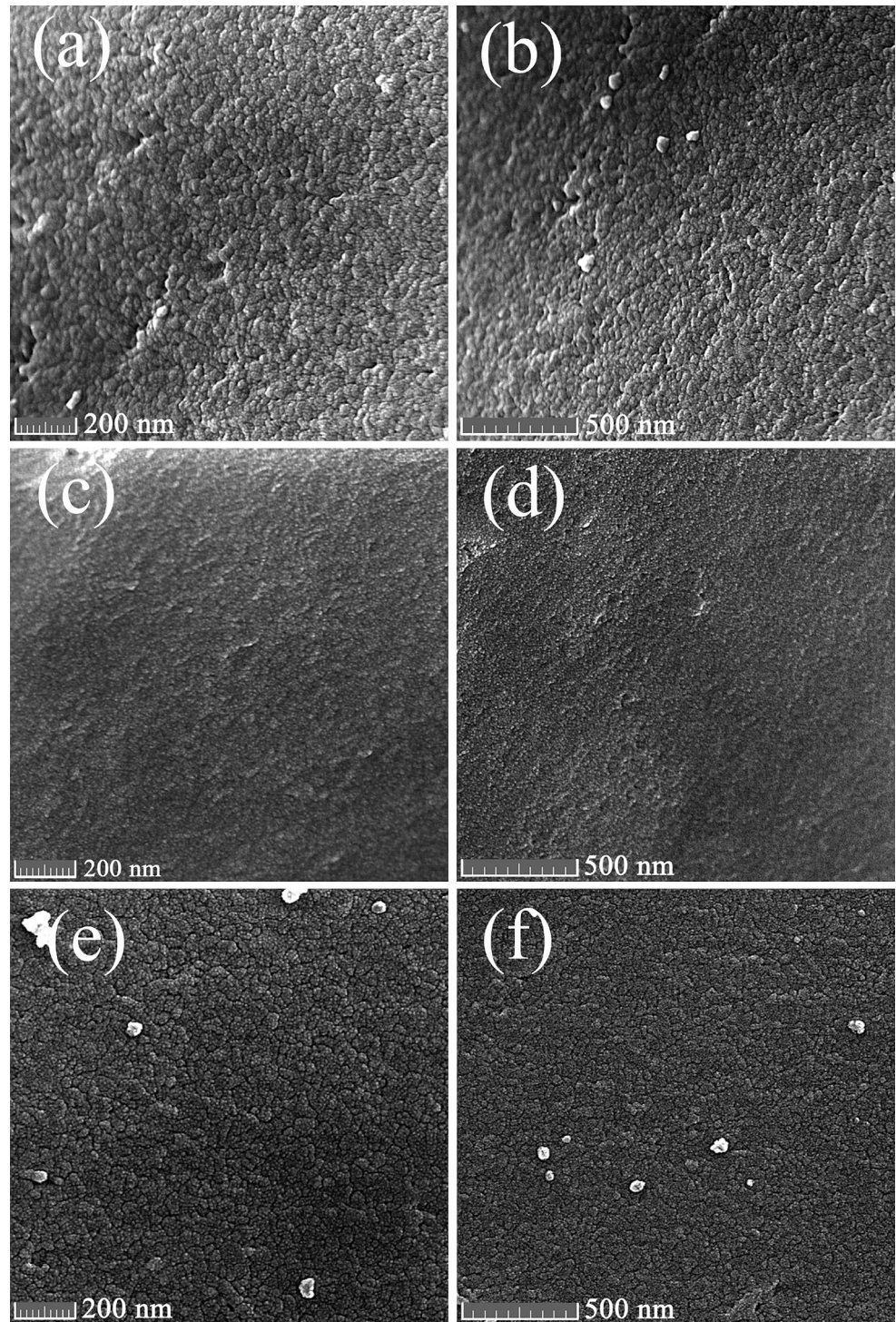
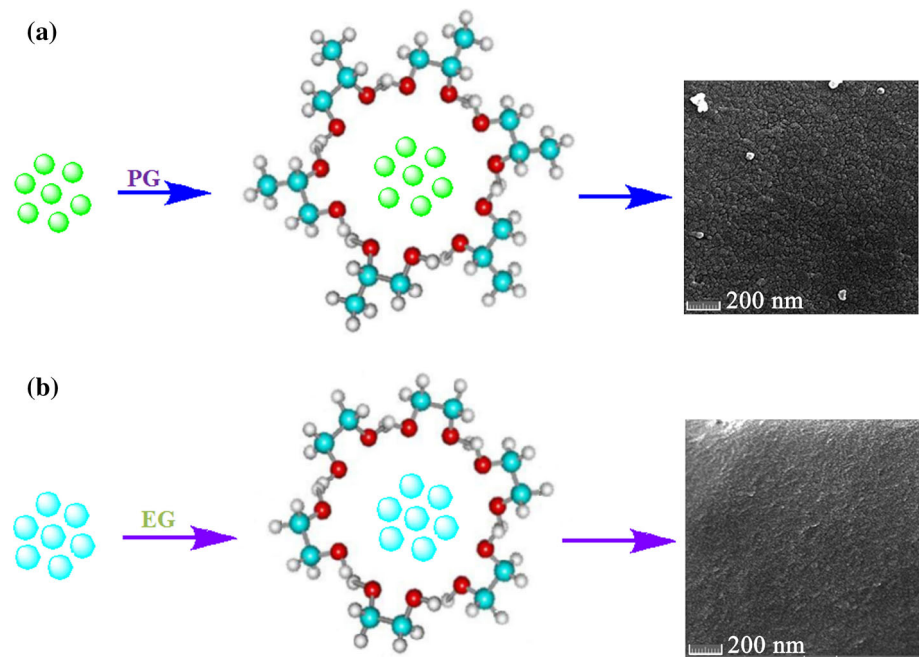


Fig. 12 Influences of **a** PG and **b** EG on shape



Acknowledgments Authors are grateful to the University of Kashan for supporting this work by Grant No. (159271/576).

References

1. S. Link, Z.L. Wang, M.A. El-Sayed, *J. Phys. Chem. B* **103**, 529 (1999)
2. S. Zinatloo-Ajabshir, M. Salavati-Niasari, *Int. J. Appl. Ceram. Technol.* **11**, 654 (2014)
3. Y. Yan, B. Sun, D.J. Ma, *J. Mater. Sci. Mater. Electron.* doi:10.1007/s10854-015-3782-9
4. B. Sun, W. Zhao, L. Wei, H. Li, P. Chen, *Chem. Commun.* **50**, 13142 (2014)
5. E.P. Marray, T. Tsai, S.A. Barnett, *Nature* **400**, 649 (1999)
6. A.V. Chadwich, *Nature* **408**, 925 (2000)
7. B.C.H. Steele, A. Heinzel, *Nature* **414**, 345 (2001)
8. N.L. Wu, S.Y. Wang, I.A. Rusakova, *Science* **285**, 1375 (1999)
9. S. Park, J.M. Vohs, R.J. Gorte, *Nature* **404**, 265 (2000)
10. V. Grover, R. Shukla, A.K. Tyagi, *Scr. Mater.* **57**, 699 (2007)
11. W. Li, H. Huang, H. Li, W. Zhang, H. Liu, *Langmuir* **24**, 8358 (2008)
12. N. Garg, V.K. Mittal, S. Bera, A. Dasgupta, V. Sankaralingam, *Ceram. Int.* **38**, 2507 (2012)
13. Q. Chang, J. Zhou, Y. Wang, G. Meng, *Adv. Powder Technol.* **21**, 425 (2010)
14. L. Kumari, G.H. Du, W.Z. Li, R.S. Vennila, S.K. Saxena, D.Z. Wang, *Ceram. Int.* **35**, 2401 (2009)
15. M. Salavati-Niasari, M. Dadkhah, F. Davar, *Polyhedron* **28**, 3005 (2009)
16. E.K. Goharshadi, M. Hadadian, *Ceram. Int.* **38**, 1771 (2012)
17. Vishwanath G. Deshmane, Yusuf G. Adewuyi, *Microporous Mesoporous Mater.* **148**, 88 (2012)
18. S. Zinatloo-Ajabshir, M. Salavati-Niasari, *J. Ind. Eng. Chem.* **20**, 3313 (2014)
19. D.V. Pinjari, K. Prasad, P.R. Gogate, S.T. Mhaske, A.B. Pandit, *Chem. Eng. Process.* **74**, 178 (2013)
20. M. Salavati-Niasari, D. Ghanbari, F. Davar, *J. Alloys Compd.* **488**, 442 (2009)
21. M. Shakouri-Arani, M. Salavati-Niasari, *J. Ind. Eng. Chem.* **20**, 3179 (2014)
22. Sh Ahmadian-Fard-Fini, M. Salavati-Niasari, F. Mohandes, *Adv. Powder Technol.* **25**, 301 (2013)
23. M. Mousavi-Kamazani, M. Salavati-Niasari, M. Sadeghinia, *Superlattices Microstruct.* **63**, 248 (2013)
24. M. Jafari, A. Sobhani, M. Salavati-Niasari, *J. Ind. Eng. Chem.* **20**, 3775 (2014)
25. S. Chandramouleeswaran, S.T. Mhaske, A.A. Kathe, P.V. Varadarajan, V. Prasad, N. Vigneshwaran, *Nanotechnology* **18**, 1 (2007)
26. A. Manikandan, N. Clament Sagaya Selvam, L. John Kennedy, R. Thinesh Kumar, J. Judith Vijaya, *J. Nanosci. Nanotechnol.* **13**, 2595 (2013)
27. A. Sobhani, M. Salavati-Niasari, *Ceram. Int.* **40**, 8173 (2014)
28. A. Sobhani, M. Salavati-Niasari, *J. Alloys Compd.* **617**, 93 (2014)
29. A. Sobhani, M. Salavati-Niasari, *J. Alloys Compd.* **625**, 26 (2015)
30. K.G. Kanade, J.O. Baeg, S.K. Apte, T.L. Prakash, B.B. Kale, *Mater. Res. Bull.* **43**, 723 (2008)
31. M. Salavati-Niasari, D. Ghanbari, M.R. Loghman-Estarki, *J. Alloys. Compd.* **488**, 442 (2009)
32. N. Clament Sagaya Selvam, A. Manikandan, L. John Kennedy, J. Judith Vijaya, *J. Colloid Interface Sci.* **389**, 91 (2013)
33. D. Ghanbari, M. Salavati-Niasari, S. Karimzadeh, S. Gholamrezaei, *J. NanoStruct.* **4**, 227 (2014)
34. G. Nabyouni, S. Sharifi, D. Ghanbari, M. Salavati-Niasari, *J. NanoStruct.* **4**, 317 (2014)
35. M. Panahi-Kalamuei, M. Mousavi-Kamazani, M. Salavati-Niasari, *J. NanoStruct.* **4**, 459 (2014)
36. F. Beshkar, M. Salavati-Niasari, *J. NanoStruct.* **5**, 17 (2015)
37. L. Nejadi-Moghadam, A. Esmaili Bafghi-Karimabad, M. Salavati-Niasari, H. Safardoust, *J. NanoStruct.* **5**, 47 (2015)